

This is an electronic reprint of the original article. This reprint may differ from the original in pagination and typographic detail.

Formulation and optimization of lyophilized nanosuspension tablets to improve the physicochemical properties and provide immediate release of silymarin

Ibrahim, AH; Rosqvist, Emil; Smått, Jan-Henrik; Ibrahim, HM; Ismael, HR; Afouna, MI; Samy, AM; Rosenholm, Jessica

Published in:
International Journal of Pharmaceutics

DOI:
[10.1016/j.ijpharm.2019.03.064](https://doi.org/10.1016/j.ijpharm.2019.03.064)

Published: 01/01/2019

Document Version
Accepted author manuscript

Document License
CC BY-NC-ND

[Link to publication](#)

Please cite the original version:

Ibrahim, AH., Rosqvist, E., Smått, J.-H., Ibrahim, HM., Ismael, HR., Afouna, MI., Samy, AM., & Rosenholm, J. (2019). Formulation and optimization of lyophilized nanosuspension tablets to improve the physicochemical properties and provide immediate release of silymarin. *International Journal of Pharmaceutics*, 563, 217–227. <https://doi.org/10.1016/j.ijpharm.2019.03.064>

General rights

Copyright and moral rights for the publications made accessible in the public portal are retained by the authors and/or other copyright owners and it is a condition of accessing publications that users recognise and abide by the legal requirements associated with these rights.

Take down policy

If you believe that this document breaches copyright please contact us providing details, and we will remove access to the work immediately and investigate your claim.

This is the accepted manuscript of [A.H. Ibrahim, E. Rosqvist, J.-H. Smått, H.M. Ibrahim, H.R. Ismael, M.I. Afouna, A.M. Samy, J.M. Rosenholm, Formulation and optimization of lyophilized nanosuspension tablets to improve the physicochemical properties and provide immediate release of silymarin. International Journal of Pharmaceutics 563 (2019) 217-227 <https://doi.org/10.1016/j.ijpharm.2019.03.064>] © 2019. This manuscript version is made available under the CC-BY-NC-ND 4.0 license <http://creativecommons.org/licenses/by-nc-nd/4.0/>”

Formulation and optimization of lyophilized nanosuspension tablets to improve the physicochemical properties and provide immediate release of silymarin.

Ahmed H. Ibrahim,^{1,2} Emil Rosqvist,³ Jan-Henrik Smått,³ Hany M. Ibrahim,^{1,4} Hatem R. Ismael,¹

Mohsen I. Afouna,¹ Ahmed M. Samy,¹ Jessica M. Rosenholm*²

¹Department of Pharmaceutics and Industrial Pharmacy, Faculty of Pharmacy, Al-Azhar University, Cairo, Egypt

²Pharmaceutical Sciences Laboratory, Faculty of Science and Engineering, Åbo Akademi University, Tykistökatu 6A, 20520 Turku, Finland

³Laboratory of Physical Chemistry, Faculty of Science and Engineering, Åbo Akademi University, Porthaninkatu 3-5, 20500 Turku, Finland

⁴Department of pharmaceutical technology, Faculty of Pharmacy, Misr International University

Abstract

Silymarin (SLM) is a hepatoprotective herbal drug characterized by low aqueous solubility and, consequently, low oral bioavailability. The objective of this study was to enhance the physicochemical properties of SLM, through preparation and optimization of lyophilized nanosuspension tablets (LNTs). LNTs were prepared by sonoprecipitation technique followed by a freeze-drying process using both polyvinyl alcohol (PVA) as stabilizer and binder, and mannitol as cryoprotectant and disintegrating agent. 3² full factorial design (FFD) was applied to study the effect of independent variables at different concentrations of both PVA (X₁) and

mannitol (X_2) on the dependent variables that included main particle size (Y_1), disintegration time (Y_2), friability % (Y_3) and time required to release 90% of the drug (Y_4). Several physicochemical evaluations were implemented on the optimized formula; for instance differential scanning calorimetry, X-ray diffractometry, Fourier transform infrared spectroscopy, scanning electron microscopy and transmission electron microscopy. These analyses demonstrated that the drug was in an amorphous state, stable in nanosize range and displayed no chemical interaction with the polymer. Moreover, the optimized formula had highly porous structure, rapid disintegration, friability with less than 1% and noticeable improvement in saturation solubility and dissolution rate.

Keywords: Silymarin; sonoprecipitation; optimization; lyophilized nanosuspension tablets

1. Introduction

Silymarin (SLM) is a polyphenolic substance extracted from fruit seeds of the milk thistle plant (*Silybum marianum*). It is composed mainly from isomers, silybin, silychristin, silydianin, isosilybin and taxifolin (Lu, Lu et al. 2007). Out of these, silybin is the major component of silymarin and the most pharmacologically active component. SLM has been widely used for treatment of various liver disorders, for instance acute and chronic viral hepatitis, cirrhosis, toxic hepatitis and fatty liver (Flora, Hahn et al. 1998, Kvasnička, Bība et al. 2003). However, the pharmacological activity of SLM is very limited due to its poor water solubility, degradation by gastric fluid, and poor permeation across intestinal epithelial cells. Therefore, SLM exhibits low dissolution rate, poor absorption and low oral bioavailability; only 23–47% of silymarin has been

This is the accepted manuscript of [A.H. Ibrahim, E. Rosqvist, J.-H. Smått, H.M. Ibrahim, H.R. Ismael, M.I. Afouna, A.M. Samy, J.M. Rosenholm, Formulation and optimization of lyophilized nanosuspension tablets to improve the physicochemical properties and provide immediate release of silymarin. International Journal of Pharmaceutics 563 (2019) 217-227 <https://doi.org/10.1016/j.ijpharm.2019.03.064>] © 2019. This manuscript version is made available under the CC-BY-NC-ND 4.0 license <http://creativecommons.org/licenses/by-nc-nd/4.0/>”

shown to be absorbed from the gastrointestinal tract after oral administration (El-Samaligy, Afifi et al. 2006, Parveen, Baboota et al. 2011, Cao, Fu et al. 2012, Elmowafy, Viitala et al. 2013).

There are different strategies that have been applied in order to improve dissolution rate and bioavailability of SLM; for instance, solid dispersions (Sun, Wei et al. 2008, Balata and Shamrool 2014), self-microemulsifying drug delivery systems (Wu, Wang et al. 2006, Li, Yuan et al. 2010), silymarin-loaded lipid microspheres (Abrol, Trehan et al. 2004), oil-based nanocarrier (Parveen, Baboota et al. 2011), complexation with cyclodextrin (Ghosh, Biswas et al. 2011), silymarin liposomes (Elmowafy, Viitala et al. 2013), silybin–phospholipid complex (Yanyu, Yunmei et al. 2006), solid lipid nanoparticles (Zhang, Liu et al. 2007, Cengiz, Kutlu et al. 2015), silymarin or dehydrosilymarinproliposome (Chu, Tong et al. 2011), and porous silica nanoparticles (Cao, Fu et al. 2012). Further, in the last two decades, nanosuspension technology has been a highlight in pharmaceutical industry and has been implemented also commercially, due to its intrinsic contribution in formulating poorly water-soluble drugs as a result of improving saturation solubility, dissolution rate and consequently the oral bioavailability (Kayaert and Van den Mooter 2012, Möschwitzer 2013). Nanosuspensions can be defined as sub-micron colloidal dispersions of nanosized pure drug particles that are stabilized by a suitable polymer, surfactant or a mixture of these; with a particle size range of 1-1000 nm (Rabinow 2004). However, nanosuspensions are unfortunately susceptible to physical instability due to high surface energy of nanocrystals that render them to be thermodynamically unstable and reinforce the risks of agglomeration and crystal growth (Ostwald ripening) (Van Eerdenbrugh, Froyen et al. 2008, Ali, York et al. 2011, Du, Li et al. 2015). Therefore, decreasing or inhibiting this crystal growth is a fundamental aspect of nanosuspension development. The use of a proper

This is the accepted manuscript of [A.H. Ibrahim, E. Rosqvist, J.-H. Smått, H.M. Ibrahim, H.R. Ismael, M.I. Afouna, A.M. Samy, J.M. Rosenholm, Formulation and optimization of lyophilized nanosuspension tablets to improve the physicochemical properties and provide immediate release of silymarin. International Journal of Pharmaceutics 563 (2019) 217-227 <https://doi.org/10.1016/j.ijpharm.2019.03.064>] © 2019. This manuscript version is made available under the CC-BY-NC-ND 4.0 license <http://creativecommons.org/licenses/by-nc-nd/4.0/>”

stabilizer and its concentration is considered one of the main factors to provide a stable nanosuspension either by steric and/or electrostatic stabilization (Du, Li et al. 2015). The stabilizer could be non-ionic polymers, for instance, hydroxypropyl methylcellulose (HPMC) (Tran, Tran et al. 2014), polyvinyl alcohol (PVA) (Morakul, Suksiriworapong et al. 2013) and polyvinylpyrrolidone (PVP) (Ibrahim, Ibrahim et al. 2018); or non-ionic surfactants, for example, poloxamer 188 and tween 80 (Ige, Baria et al. 2013, Morakul, Suksiriworapong et al. 2013) or ionic surfactants such as sodium lauryl sulfate (SLS) (Mahesh, Singh et al. 2014). Nanosuspensions are generally produced by either top-down method (media milling or high-pressure homogenization) or bottom up method (nanoprecipitation) (Dening, Rao et al. 2016). Nanoprecipitation is the most common method due its simplicity and cost-effectiveness. Moreover, ultrasonication could be combined with nanoprecipitation method to enhance the reduction of particle size during displacement process and to control the processes of nucleation and crystallization (Sinha, Müller et al. 2013). Drying of nanosuspensions is an intrinsic factor in the stabilization of drugs in nanosize range. The drying process could be performed by different methods, for example using a spray drier or freeze drier. Freeze-drying or lyophilization is a dehydration process that is used to preserve the particles of the drug in a stable nanosize range and to improve the long term stability of the nanoparticles and, consequently, simplifying its handling and storage (Abdelwahed, Degobert et al. 2006b). Freeze-drying process includes three steps: freezing, primary drying (removing of the water from the frozen formula by sublimation of the ice) and secondary drying (desorption of unfrozen water under vacuum) (Abdelwahed, Degobert et al. 2006b). The freeze-drying process may negatively affect the stability of nanoparticles as a result of freezing stress and desiccation stress, due to that during the freezing

This is the accepted manuscript of [A.H. Ibrahim, E. Rosqvist, J.-H. Smått, H.M. Ibrahim, H.R. Ismael, M.I. Afouna, A.M. Samy, J.M. Rosenholm, Formulation and optimization of lyophilized nanosuspension tablets to improve the physicochemical properties and provide immediate release of silymarin. International Journal of Pharmaceutics 563 (2019) 217-227 <https://doi.org/10.1016/j.ijpharm.2019.03.064>] © 2019. This manuscript version is made available under the CC-BY-NC-ND 4.0 license <http://creativecommons.org/licenses/by-nc-nd/4.0/>”

process, there is separation of phases into ice and cryoconcentrated suspension that contain a high concentration of nanoparticles that, in turn, lead to agglomeration of the particles.

Moreover, a mechanical stress to the nanoparticles may be imparted by ice crystallization and consequently, instability of the nanoparticles. Furthermore, the primary drying should be applied below the collapsed temperature (TC) to avoid product collapse (Fonte, Reis et al. 2016) (Abdelwahed, Degobert et al. 2006b). To avoid these issues, different excipients could be added as cryoprotectants and lyoprotectants before the lyophilization process (Sinha, Müller et al. 2013, Fonte, Reis et al. 2016). Sugars are considered the most common cryoprotectants; for instance mannitol (Ige, Baria et al. 2013), trehalose and sucrose (Ćurić, Keller et al. 2015). Polymers could also be used as cryoprotectants, such as PVP and PVA (Abdelwahed, Degobert et al. 2006a). In this study, the nanosuspension technique was applied using sonoprecipitation method and integrated with lyophilized tablet for formulation and optimization of a promising lyophilized nanosuspension tablet (LNT) of SLM using PVA and mannitol. The optimization process was applied using the concentration of both polymer (polyvinyl alcohol, PVA) and mannitol as independent variables. PVA acted as both stabilizer for stabilization of the nanosuspension and binder for the formation of the lyophilized tablet, and mannitol was used as cryoprotectant and lyoprotectant for inhibition of nanoparticles aggregation, as well as disintegrating agent for the lyophilized tablet. Moreover, mannitol is characterized by being freely water soluble, non-hygroscopic and providing a cooling sensation in the mouth (Wilku, McNeil et al. 2017). Here, the formulation was performed in one-step by adjusting the concentration of polymer that act as stabilizer and binder for the preparation of the nanosuspension, without the need for subsequent tablet compression that would, most likely,

This is the accepted manuscript of [A.H. Ibrahim, E. Rosqvist, J.-H. Smått, H.M. Ibrahim, H.R. Ismael, M.I. Afouna, A.M. Samy, J.M. Rosenholm, Formulation and optimization of lyophilized nanosuspension tablets to improve the physicochemical properties and provide immediate release of silymarin. International Journal of Pharmaceutics 563 (2019) 217-227 <https://doi.org/10.1016/j.ijpharm.2019.03.064>] © 2019. This manuscript version is made available under the CC-BY-NC-ND 4.0 license <http://creativecommons.org/licenses/by-nc-nd/4.0/>”

affect the nanoparticles e.g. in terms of size. Therefore, formulation of LNTs of SLM is the best approach for not only providing rapid disintegration, higher saturation solubility and faster dissolution rate than other nanoparticle-based techniques.

2. Materials and methods

2.1. Materials

Silymarin (SLM), polyvinyl alcohol (PVA, Mowiol[®]20-98), absolute ethanol, tween 80 and sodium chloride were purchased from Sigma–Aldrich, Inc.(St.Louis, Missouri). Mannitol, Potassium dihydrogen phosphate and Calcium chloridewere purchased from Merck (Merck KGaA, Darmstadt, Germany). Sodium hydroxide was purchased from VWR chemical (VWR, Geldenaaksebaan, Leuven, Belgium).

2.2. Methods

Preparation of lyophilized nanosuspension tablet (LNT) of silymarin

Silymarin nanosuspensions were prepared by sonoprecipitation method with slight modification(Tran, Tran et al. 2014). Briefly, Silymarin (250mg) was dissolved in the least volume of absolute ethanol (1.5 ml)(Li, Yuan et al. 2010). Antisolvent phase was prepared by dissolving both PVA and mannitol in water and cooled in an ice water bath. Then the obtained drug solution was quickly injected into the antisolvent phase during stirring with magnetic stirrer at 750 rpm followed by ultrasonication using adaptive focused acoustic energy (Covarissonicator S2, Massachusetts, USA) at fixed parameter, 4 °C and acoustic power 24 W for 120 second distributed on 2 cycles. The resulting nanosuspensions were quickly poured into the pockets of a

This is the accepted manuscript of [A.H. Ibrahim, E. Rosqvist, J.-H. Smått, H.M. Ibrahim, H.R. Ismael, M.I. Afouna, A.M. Samy, J.M. Rosenholm, Formulation and optimization of lyophilized nanosuspension tablets to improve the physicochemical properties and provide immediate release of silymarin. International Journal of Pharmaceutics 563 (2019) 217-227 <https://doi.org/10.1016/j.ijpharm.2019.03.064>] © 2019. This manuscript version is made available under the CC-BY-NC-ND 4.0 license <http://creativecommons.org/licenses/by-nc-nd/4.0/>”

PVC blister pack to attain silymarin dose of 50 mg per tablet. The tablet blister packs were then transferred to a freezer at -80°C and kept for 6 h. Then the frozen tablets were freeze dried for 24 h. using Hetotrap CT 60e lyophilizer (Heto-HoltenA/S, Allerød, Denmark). The obtained lyophilized nanosuspension tablets (LNTs) were kept in tightly closed amber yellow containers at room temperature until further use.

2.3. Experimental design and optimization

A 3² full factorial design (FFD) was applied to study the effect of independent variables (factors) on dependent variables (responses) to obtain optimized formula of LNT. In this design, there were two independent variables: X₁, concentration of PVA and X₂, concentration of mannitol that chosen after Preliminary studies. The dependent variables are mean particles size after lyophilization (Y₁), Disintegration time (Y₂), friability % (Y₃) and time required to release 90 % of SLM, T90 (Y₄). The effects of independent variables were studied at three actual and coded levels as elucidated in the table 1. The higher, lower and the intermediate levels of each factor are coded as +1, -1 and 0, respectively.

3² FFD was generated by Design-Expert 10.0 software that provided the best fitting model for comparison for several statistical parameters, including the regression coefficient (R²), analysis of variance so that all analyses could be applied for nine batches. The mathematical model equation that represents 3² FFD is the following quadratic equation:

$$Y = \beta_0 + \beta_1 X_1 + \beta_2 X_2 + \beta_3 X_1 X_2 + \beta_4 X_1^2 + \beta_5 X_2^2 \quad (1)$$

Y is the measured response (independent variable), while β_0 is the intercept, β_1 to β_5 are the regression coefficient for the second order polynomial equation and X_1 & X_2 represents the main effects (independent variables). $X_1 X_2$ represents the interaction between the main effects.

X_1^2 & X_2^2 are quadratic terms of independent variables that were used to simulate the curvature of the designed sample space. For visualizing the significant effect of independent variables the 3-dimensional graphs of response surface were applied. The optimized LNT was formulated based on the constraints on both independent variables and dependent variables where the goal was to minimize the all responses as elucidated in table 1. Then to validate the suggested optimized LNT, the experimental observed values of the responses were quantitatively compared with the predicted values by the mathematical models furthermore; the relative error (%) was calculated using the following equation:

$$\text{Relative error (\%)} = \left(\frac{\text{Predicted value} - \text{Experiment value}}{\text{Predicted value}} \right) \times 100 \quad (2)$$

2.4. Characterizations of lyophilized nanosuspension tablet of Silymarin.

2.4.1. Mean Particle size, zeta-potential and poly polydispersity index (PdI)

The particle size before and after lyophilization, PdI and Zeta-potential of LNTs were measured using dynamic light scattering zetasizer (Nano ZS, Malvern Instruments Limited,

Worcestershire, UK). Each sample was suitably suspended with Milli-Q water before analysis.

Each sample was analyzed in triplicate and the results were recorded as the mean value of these runs \pm SD.

2.4.2. In vitro disintegration test

According to FDA guidelines, the disintegration test could be applied using the conventional disintegration testing (McLaughlin, Banbury et al. 2009). Therefore, the in vitro disintegration test was applied according to USP32- NF27 requirements for uncoated tablets using Disintegration Tester (Sotax DT2, Basel, Switzerland) . The disintegration time for the all prepared LNT included optimized formula were determined in the dissolution medium maintained at $37 \pm 0.5^{\circ}\text{C}$. Six tablets from each batch were randomly chosen to determine the disintegration time. All results were recorded as mean value \pm SD (n = 6)

2.4.3. Friability test

Friability test provides an indication about the strength of the tablet and its ability to withstand the abrasion during handling, packaging and shipment. The friability test for all batches and optimized formula were examined using Roche friabilator USP test apparatus (Erweka Friability Testers Type TA, GMBH, Germany). Ten lyophilized tablets for each batch were weighed (initial weight) then rotated in the apparatus at 25 rpm for 4 min. The tablets were then removed, dedusted and reweighed to determine the final weight their weight was determined. % friability was calculated as follows:

$$\text{Friability \%} = \frac{\text{Initial weight} - \text{Final weight}}{\text{Initial weight}} \times 100 \quad (3)$$

2.4.4. Mechanical strength testing

The tablet strength was evaluated for the nine formulae and the optimized formula. The tablet showed plastic deformation so that a Texture analyzer (Stable Micro System, United Kingdom) was used, equipped with exponent Stable Micro System software (Corveleyn and Remon 1997). A 2 mm flat surface probe was used, the tablet was placed on a support and applied force with speed 2mm/sec was used to penetrate 2 mm depth into the tablet. The maximum force could be displayed using exponent software.

2.4.5. Dissolution study

The in vitro release study was conducted using USP Apparatus I (SOTAX AT 7 smart, Allchwil/Basel, Switzerland) it was applied for pure SLM, nine batches and the optimized formula. 1000 ml of simulated salivary fluid (pH 7.4)(Gittings, Turnbull et al. 2014) containing 0.5 % Tween 80 was selected as dissolution medium. The temperature was maintained at 37°C ± 0.5 °C and a stirring rate of 100 rpm. The tablet equivalent to 50 mg silymarin was placed inside the basket in the dissolution vessel. Samples of 2 ml were withdrawn in predetermined time intervals and replenished by an equal volume of the fresh dissolution medium. All samples were filtered using 0.2 µm syringe filter (VWR, Leuven), and analyzed spectrophotometrically (Lambda 35 UV/VIS Spectrophotometer, PerkinElmer, Singapore) at wavelength 288 nm. All experiments were run in triplicates to determine the mean value and standard deviation (SD).

2.4.6. Drug content study

Ten tablets of optimized formula were finely powdered and blended. A quantity equivalent to 50 mg of SLM was weighed and dissolved in the dissolution medium under continuous stirring. The solutions were filtered using 0.2 µm syringe filter (VWR, Leuven) and the drug content was determined spectrophotometrically at 288 nm (Lambda 35 UV/VIS Spectrophotometer, PerkinElmer, Singapore). The measurements were repeated three times to determine the mean value and standard deviation (SD). Drug content percent could be calculated using the following equation:

$$\text{Drug content \%} = \frac{\text{Concentration of drug measured}}{\text{Initial concentration of drug originally added}} \times 100 \quad (4)$$

2.4.7. Saturation solubility study

An excess amount of pure SLM and optimized LNT were dispersed in the dissolution medium and placed on a shaker (Shaking Water Bath SW22, JULABO GmbH, Germany) at 37 °C ± 0.5 °C. The shaking was held on till the solubility equilibrium had been reached. Samples were filtered through 0.2 µm syringe filter (VWR, Leuven). Then the concentration of SLM was spectrophotometrically analyzed (Lambda 35 UV/VIS Spectrophotometer, PerkinElmer, Singapore) at 288 nm. The measurements were repeated three times. In addition, one-way ANOVA test was carried out to detect the significant difference (*p* value) between pure drug and optimized LNT.

This is the accepted manuscript of [A.H. Ibrahim, E. Rosqvist, J.-H. Smått, H.M. Ibrahim, H.R. Ismael, M.I. Afouna, A.M. Samy, J.M. Rosenholm, Formulation and optimization of lyophilized nanosuspension tablets to improve the physicochemical properties and provide immediate release of silymarin. International Journal of Pharmaceutics 563 (2019) 217-227 <https://doi.org/10.1016/j.ijpharm.2019.03.064>] © 2019. This manuscript version is made available under the CC-BY-NC-ND 4.0 license <http://creativecommons.org/licenses/by-nc-nd/4.0/>”

2.4.8. Scanning Electron Microscopy

Scanning electronic microscopy (SEM) images were studied for cross-section and surface of optimized LNT using SEM instrument (LEO 1530 SEM Oberkochen, Germany). The sample was mounted in resin followed by rough grind and polishing of the opposite side to be flat that aim the sample to stick easily on the plate specimen. The sample was coated with carbon to improve the electrical conductivity before examination. The sample was viewed at different magnifications.

2.4.9. Transmission Electron Microscopy

The surface morphology of the optimized LNT was visualized by transmission electron microscope (TEM) (Jeol JEM-1400 plus TEM, Tokyo, Japan). The optimized LNT was redispersed in distilled water. Briefly, a drop of the resulted dispersion was placed onto carbon-coated copper grids. Then the grid was air dried, and viewed under different magnifications.

2.4.10. Differential Scanning Calorimetry (DSC)

The DSC thermograms of pure silymarin, optimized LNT, PVA, Mannitol and physical mixture of SLM, PVA and mannitol were recorded using DSC apparatus (DSC Q2000, TA Instruments—Waters LLC, New Castle, Delaware, US). Approximately 1–2 mg of fresh sample was taken in an aluminium pan and crimped on lids using a press. Samples were heated at scanning rate of 10 °C/min in the range of 30 to 300 °C in presence of nitrogen at flow rate of 40 ml/min to obtain the endothermic peaks.

This is the accepted manuscript of [A.H. Ibrahim, E. Rosqvist, J.-H. Smått, H.M. Ibrahim, H.R. Ismael, M.I. Afouna, A.M. Samy, J.M. Rosenholm, Formulation and optimization of lyophilized nanosuspension tablets to improve the physicochemical properties and provide immediate release of silymarin. International Journal of Pharmaceutics 563 (2019) 217-227 <https://doi.org/10.1016/j.ijpharm.2019.03.064>] © 2019. This manuscript version is made available under the CC-BY-NC-ND 4.0 license <http://creativecommons.org/licenses/by-nc-nd/4.0/>”

2.4.11. Powder X-ray Diffraction (PXRD)

Powder x-ray diffraction measurements were applied for the all samples as in the DSC measurements. PXRD was carried out with a Bruker D8 Discover instrument (Karlsruhe, Germany) equipped with a Cu K α x-ray source and scintillator point detector. The samples were scanned in the 2-theta range of 10-30° using a step size of 0.04° for 4 s per step.

2.4.12. Attenuated Total Reflection Fourier Transform Infrared Spectroscopy (ATR-FTIR)

Attenuated total reflectance Fourier transform infrared (ATR-FTIR) spectra were recorded for the all samples used for DSC. ATR-FTIR was applied using a Spectrum two spectrophotometer (UTAR-FTIR spectrophotometer, PerkinElmer, Llantrisant, UK). The samples were placed on a diamond crystal then the spectra recorded at 100 scans and at 4 cm⁻¹ resolution over the wavenumber region 4000–650 cm⁻¹.

2.4.13. Stability study

The stability for the optimized LNTs was studied according to FDA guidelines (FDA 2003) by combining the criteria for accelerated (humidity) and long-term (temperature, time) stability testing. Thus, the LNTs were stored in desiccator at 25 °C with maintaining the relative humidity at 75 % using a saturated solution of sodium chloride. Samples were taken at 0, 1, 2, and 3, 6 and 12 months storage to evaluate particle size, dissolution, drug content, disintegration and friability. One-way ANOVA test was used to analyze the mean \pm SD of the results.

3. Results and Discussion

3.1. Analysis of Data and Experimental Design Optimization

Preliminary investigations for different hydrophilic polymers PVA, PVP, HPMC, HPC and HEC showed obvious agglomeration of the particles for PVP, HPMC, HPC and HEC, while there was no agglomeration of the particles for PVA. Therefore, PVA was selected for further studies. All results of the 9 prepared batches are presented in Table 1. The concentration of both PVA and mannitol were independent variables, and used to study their effect at various levels on the dependent variables (mean particle size, dissolution rate, disintegration time and friability %). Design expert 10 software provided multiple regressions to yield suitable second polynomial model equations as follows:

Y_1 (Particle size)

$$= 881.631 - 336.471X_1 - 68.777X_2 + 66.333X_1^2 + 5.988X_1X_2 + 3.723X_2^2 \quad (5)$$

Y_2 (Disintegration time)

$$= -36.696 + 56.985X_1 - 4.448X_2 + 0.867X_1^2 - 6.044X_1X_2 + 0.982X_2^2 \quad (6)$$

Y_3 (Friability %)

$$= 8.050 - 7.353X_1 + 0.780X_2 + 1.575X_1^2 - 0.234X_1X_2 - 0.012X_2^2 \quad (7)$$

Y_4 (T90)

$$= 62.472 - 41.310X_1 - 3.067X_2 + 12.283X_1^2 - 0.581X_1X_2 + 0.19X_2^2 \quad (8)$$

ANOVA was also applied (Table 2) to demonstrate the significant effects of the main variables (X_1 and X_2) and their interaction on the responses (Y_1 , Y_2 , Y_3 and Y_4).

3.1.1. Effect of the independent variables on the particle size after lyophilization (Y_1)

Nanosuspensions are thermodynamically unstable, have high total surface energy (extra Gibbs free energy) so that improper concentration of stabilizer may lead to agglomeration of nanoparticles in order to minimize this surface energy. This agglomeration may also contribute to crystal growth (Ostwald ripening) as a result of agglomeration of smaller particles. Ostwald ripening is a phenomenon in which smaller particles have higher saturation solubility than larger particles, and consequently diffusion of the drug molecule occurs from the higher concentration surrounding the smaller particles to the area with low drug concentration surrounding the larger particles that, in turn, result in crystallization of the drug on the large particles. In other words, coarse particles grow at the expense of small particles that in turn increase the particle size and particle size distribution in order to reach a more thermodynamically stable state (Ali, York et al. 2011, Merisko-Liversidge and Liversidge 2011, Du, Li et al. 2015). However, the mean particle size after lyophilization (Y_1) ranged from 269.7 ± 1.8 nm to 546.5 ± 68.4 nm as presented in Table 1 and 3D graph of response surface (Figure 1a). The effect of both independent variables and their interaction on Y_1 could be elucidated as follows: At fixed concentration of X_2 at any level, Y_1 was significantly decreased when the concentration of PVA was increased from 1 % w/v to 2 % w/v and increased when the concentration was increased from 2 % w/v to 3 % w/v. The significant improvement in the particle size reduction (after lyophilization) by increasing the

concentration of PVA could be demonstrated in table 2 ($p < 0.05$) and that may be due to the following reasons. First, PVA is a nonionic polymer that provided steric repulsion between the particles as a result of formation of a hydrodynamic boundary layer that surrounded the nanoparticles, which could be observed in TEM. Therefore, the agglomeration and crystal growth (Ostwald ripening) was inhibited based on the optimized concentration of PVA that provided a complete adsorption of stabilizer on the crystal surface, that reduced surface free energy and maintained the lowering particle size distribution (Rana and Murthy 2013, Sinha, Müller et al. 2013, Du, Li et al. 2015). Moreover, the particle size may be stabilized due to the high affinity of the polymer for the particle surface through formation of hydrogen bonds between stabilizer and the drug molecule, which could be determined via FTIR spectra. Furthermore, PVA could act as cryoprotectant and maintain the homogeneity of particles in nanosize range during the freezing process (Fonte, Reis et al. 2016, Malamatari, Somavarapu et al. 2016). However, at low concentration of PVA, there was insufficient coverage on the surface of the crystal by stabilizer that led to inefficiency in decreasing the high surface energy and, consequently, generated agglomeration of the nanoparticles after lyophilization (Ali, York et al. 2011, Brough and Williams Iii 2013, Sinha, Müller et al. 2013). These results were in agreement with the results of mean particle size before lyophilization as elucidated in Table 3, in which at low concentration of PVA, at any level of X_2 , the particle size for N1, N4 and N7 were significantly increased after lyophilization. While at 2% w/w of PVA, at any level of X_2 , the particle size for N2, N5 and N8 were slightly increased (particularly N5 and N8) after lyophilization when compared with N1, N4 and N7, respectively, which demonstrated the insufficient coverage on the surface of the crystal at low concentration of PVA and,

consequently, increase the particle size after the lyophilization process. While at high concentration of stabilizer, the viscosity of the solution was elevated which hindered the transmission of ultrasonic energy and consequently, hampered the diffusion during antisolvent displacement which in turn lead to significantly increase the particle size and hence, crystal growth (Ostwald ripening) (Verma, Lan et al. 2009, Brough and Williams Iii 2013, Sinha, Müller et al. 2013). These results were in agreement with the results of mean particle size before the lyophilization process as demonstrated in Table 3, in which at high concentration of stabilizer, at any level of X_2 , the mean particle sizes before and after lyophilization for N3, N6 and N9 were higher than that for N2, N5 and N8, respectively. On the other hand, at fixed concentration of X_1 at any level, Y_1 was significantly decreased ($p < 0.05$) when the concentration of mannitol was increased from 1% w/v to 9% w/v. The reduction of the particle size may be due to that mannitol minimized the lyophilization stress (lyoprotectant), reduced the mechanical stress of ice crystallization during freezing step (cryoprotectant) and prevented aggregation through providing a protective glassy matrix. Moreover, the optimized concentration of mannitol provided a freeze-dried cake with porous structure that easily resuspended and finally preserved the particles size distribution within the nanosize range. These results were in agreement with the results of the mean particle size before lyophilization, which demonstrated that the mannitol had no effect on the particle size before lyophilization while it had a significant effect (acted as cryoprotectant and lyoprotectant) after lyophilization (Fonte, Reis et al. 2016, Malamatar, Somavarapu et al. 2016).

3.1.2. Effect of independent variables on Disintegration time (Y_2)

According to USP, the disintegration time of oral disintegrating tablet is lower than 3 minutes.

Disintegration time was determined for all batches of LNT and the optimized formula. It ranged from 1.6 ± 0.4 second to 125.0 ± 4.1 seconds, and all results are summarized in Table 1. The results could be analyzed using 3 D graph of response surface in Figure 1b as follows: fast disintegration of LNTs due to highly porous structure of the tablets, as a result of sublimation of frozen water during lyophilization process that led to formation of tablet with highly porous structure. Therefore, water penetrates easily via LNT and provides rapid disintegration.

Moreover, at fixed concentrations of X_1 , the higher the concentration of mannitol, the faster the disintegration of LNT due to that mannitol decreased the binding effect of the PVA and facilitated the redispersion of LNT (Mou, Chen et al. 2011, Fonte, Reis et al. 2016). On the other hand, at fixed levels of X_2 , long time for disintegration of LNT was observed when the concentration of the PVA was increased. This is due to that PVA has adhesive properties and could act as binder, and when increasing the concentration, this yielded firm tablets with long disintegration time (Higuchi, Tanaka et al. 2014).

3.1.3. Effect of independent variables on the friability % (Y_3)

According to USP, friability % of tablets should be lower than 1%. Friability % was measured for all batches of LNT according to the optimized formula and ranged from 0.08% to 6.3 % as displayed in Table 1 and Figure 1c. At low concentration of PVA, when the concentration of mannitol was increased, the tablet started to be more friable as the mannitol obviously decreased

the binding effect of PVA at low concentration of X1. When the concentration of PVA was increased (2% w/v), the tablet started to be less friable due to the binding effect of the PVA. While at high concentration of PVA, the change in the concentration of mannitol will not affect the friability of the tablet, which could be observed in Table 2 in which the interaction between the main effects (X1X2) had a significant effect on the friability ($p < 0.05$). On the other hand, the mechanical strength of tablets were examined for nine formulae and it was observed that an increase in the concentration of both PVA and mannitol led to enhanced strength of the tablet, which is due to PVA acting as a binder while the mannitol induced tablet rigidity (McLaughlin, Banbury et al. 2009, Wilkhu, McNeil et al. 2017). On the other hand, although mannitol increased the strength of the tablet, the disintegration was still rapid with increased concentration. This is owing to that after lyophilization of mixtures of mannitol and PVA, the mannitol converted to the amorphous form (δ -form) which was confirmed by DSC and PXRD results of blank lyophilized tablets, in which also the characteristic endothermic peak of the PVA disappeared (Higuchi, Tanaka et al. 2014, Kulkarni, Suryanarayanan et al. 2018). This finally increases the wettability of the tablet with high concentration of amorphous form of mannitol, which in turn led to rapid disintegration and consequently, fast dissolution.

3.1.4. Effect of the independent variables on T90 (Y_4)

Dissolution studies were applied for pure SLM and all batches of LNT. Pure SLM shows slow dissolution rate as illustrated in Figure 2, due to poor aqueous solubility and large crystal size, which was confirmed through its characteristic peaks using both PXRD and DSC. T90 for the

nine batches of LNT ranged from 7.1 ± 0.2 min to 44.2 ± 3.8 min while for the optimized formula, the T90 was 8.9 min, as presented in Figure 2. The nine batches of LNTs and the optimized LNT demonstrated rapid dissolution rate due to the following reasons. At fixed level of X_2 , T90 decreased when the concentration of PVA was increased from 1 %w/v to 2 %w/v and started to be elevated when the concentration of PVA was increased from 2 %w/v to 3 %w/v, as elucidated in Table 3 and response surface 3D graph (Figure 1d). This enhancement may be due to the significant effect of both PVA and mannitol on the T90 ($p < 0.05$), as elucidated in the analysis of variance in Table 2. PVA is a hydrophilic polymer that enhance the wettability of SLM and hence, increase the dissolution rate. Moreover, PVA reduce the particle size of SLM as previously mentioned, which resulted in increased surface area and consequently, enhanced dissolution rate. Finally, the highly porous structure of tablets aided in the rapid disintegration and accordingly, the dissolution rate was remarkably enhanced. While at high concentration of PVA, the dissolution rate was slow (T90 was increased) due to high concentration of polymer. Particularly higher molecular weight generally leads to an increase in the thickness of the diffusion layer, which led to formation of a gel that entrapped the drug due to the high molecular weight of PVA and, correspondingly, a decrease the dissolution rate. At fixed level of X_1 , the higher the concentration of mannitol the faster the rate of dissolution, as displayed in Figure 1. This is due to that an increased concentration of mannitol helps to avoid the formation of collapsed cake, and provides fast redispersibility of the LNT in a short time. Moreover, mannitol acted as cryoprotectant and lyoprotectant, contributed in maintaining the particles in nanosize that resulted in excessively enhancing the dissolution rate.

3.1.5. Model validation

Design Expert software could recommend the optimum concentration of both independent variables that had the highest desirability approximately equal to 1, as illustrated in Figure 3a. The optimum concentrations of independent variables for preparation of optimized LNT were 2.33 % w/v and 9.0 % for PVA and mannitol, respectively; while the weight of the optimized LNT is 186.0 mg that composed of 50 mg SLY, 28.0 mg PVA and 108.0 mg mannitol. The observed (actual) value for responses were measured and displayed for the optimized formula as follows: Y_1 of 277.3 ± 10.4 nm, Y_2 of 14.0 ± 2.2 sec., Y_3 of 0.59 ± 0.07 % and Y_4 of 8.9 ± 0.6 min while the predicted (theoretical) values as follow: Y_1 of 266.2 nm, Y_2 of 13.6 sec., Y_3 of 0.57 % and Y_4 of 8.6 min. All results demonstrated that the observed and the predicted results were in close agreement. Moreover, the relative error percentage between the observed and the predicted values less than 5% as elucidated in Table 4 confirmed the reproducibility and validity of the developed models.

3.2. Characterization of optimized LNT

The optimized LNTs had proper appearance (Figure 3b); and particle size, zeta potential, PDI, drug content and mechanical strength were 277.3 ± 10.4 nm, -22.8 ± 2.8 mV, 0.114 ± 0.075 , 96.8 ± 1.85 % and 490.8 ± 22.2 g, respectively. Although zeta potential was not very high, the optimized LNT was colloidally stable due to the steric stabilization provided by the nonionic polymer (PVA) that form a hydrodynamic layer surrounding the particles, as also observed in the TEM image. Moreover, the PDI was significantly lower than 0.3, which confirmed the narrow size distribution of the sample (Wang, Liu et al. 2011). Finally, the particles were in a stable

nanosize range based on the effect of both independent variables; in addition, the ultrasonic homogenization provided complete adsorption of PVA on the drug molecules that resulted in restraint of the drug from diffusing back into the bulk and thus prevented drug precipitation. Accordingly, the drug content was maintained high. The saturation solubility results of pure SLM and optimized LNT were 1324.3 mg \pm 5.74 mg and 4616.1 mg \pm 11.02 mg, respectively. This significant difference is due to that in the optimized LNT, the surface area of SLM was exceedingly increased as a result of reducing its particle size which, in turn, enhanced the solubility. Moreover, PVA is a hydrophilic polymer that aided in the wettability of the drug and hence, the aqueous solubility was exceedingly improved.

3.2.1. Scanning Electron Microscopy

SEM was applied for optimized LNT as presented in Figure 4. SEM micrograph from surface view (Figure 4a) and cross section (Figure 4b) demonstrated the highly porous structure of optimized LNT. The freeze-drying step is responsible for the sublimation process of the frozen water, yielding a tablet of high porosity. Therefore, this highly porous nature facilitates the penetration of water into the tablet and accordingly rapid disintegration (Corveleyn and Remon 1997). Furthermore, after applying high magnification for SEM micrograph of optimized LNT (Figure 4c), it can be seen that the particles size was maintained in nanosize range, which provided greater surface area thereby extremely enhancing the dissolution rate after rapid disintegration.

3.2.2. Transmission Electron Microscopy

TEM was applied for optimized LNT as shown in Figure 4d. TEM micrographs showed spherical shape with dimensions similar or slightly lower than those resulted from DLS. This

difference may be due to DLS technique based on intensity and can record the hydrodynamic diameter of nanoparticles in suspension only. In contrast, TEM technique is based on number, the sample was dried under ultrahigh vacuum conditions and TEM provides the projected surface area based on how much of the incident electrons were transmitted through the sample.

Therefore, the size resulted from DLS is usually bigger than TEM (Bhattacharjee 2016). TEM micrograph also showed the prospective hydrodynamic layer of PVA that surrounds the nanoparticles of the drug, which demonstrates that the stabilizer had good affinity for the particle surface and provided steric stability in suspension form.

3.2.3. Differential scanning calorimetry

DSC thermograms of pure SLM, PVA, mannitol, physical mixture1 (mixing of pure SLM, mannitol and PVA), blank (lyophilized tablet without SLM), physical mixture2 (mixing of pure SLM with blank) and optimized LNT are presented in Figure 5. Pure SLM had a broad endothermic peak at 75°C and endothermic peak at 146°C, which represent the melting points of pure SLM and its crystalline nature (Lian, Lu et al. 2011, Cao, Fu et al. 2012). While PVA and mannitol had the characteristic peaks at 217°C and 168°C, respectively (Gil, Barreneche et al. 2013, Solé, Neumann et al. 2014). DSC thermogram of physical mixture1 exhibited that SLM existed in crystalline state due to the presence of its characteristic peaks, and there was no change in the endothermic peaks of both PVA and mannitol. On the other hand, the thermogram of blank (lyophilized tablet without SLM) showed there was a large endothermic peak of mannitol at 156°C that represented the δ -form, and a small endothermic peak at 167°C that represented the β -form. The presence of these two peaks could explain the transition between δ and β -forms during lyophilization process of solution of mannitol with PVA (Burger, Henck et

al. 2000, De Waard, Hinrichs et al. 2008, Barreneche, Gil et al. 2013, Higuchi, Tanaka et al. 2014). While the endothermic peak of PVA disappeared, this demonstrated the amorphous form of PVA and formation of hydrogen bonds between PVA and mannitol (Higuchi, Tanaka et al. 2014). The thermograms of the physical mixture² and optimized LNT were similar to the blank due to the overlap of the characteristic peak of the drug (148°C) with the characteristic peak of δ -form (155°C). Therefore, DSC could not efficiently detect if the drug in the formula is still in crystalline state or changed partially or completely to amorphous state. Therefore, PXRD was applied to determine the crystallinity of the drug in optimized LNT.

3.2.4. Powder X-ray Diffraction

PXRD patterns of pure SLM, PVA, mannitol, physical mixture¹, physical mixture², blank and optimized LNT are shown in Figure 6. Pure SLM has distinctive peaks in the 2θ range of 13-28° as well as a broad hump centered at about 20°. These features originate from the crystalline and amorphous portions of silymarin, respectively. The mannitol reference sample consists predominantly of the β polymorph of D-mannitol (Mehta, Bhardwaj et al. 2013), while some of the δ can also be detected. A similar pattern can also be seen for physical mixture¹. Furthermore, in the physical mixture¹, the semicrystalline features of PVA (i.e. three broad reflections at 11.4°, 19.6°, and 22.8°) can be observed superimposed over the sharp silymarin and mannitol peaks. Four of the SLM peaks (13.7°, 14.6°, 16.1°, and 17.3°) can be identified in the two physical mixture samples (the rest of the silymarin reflections are overlapping with the mannitol peaks), demonstrating that they contain crystalline silymarin. However, none of these peaks could be identified in the optimized LNT sample highlighting that the drug is amorphous in the lyophilized sample. However, both the blank and the physical mixture² samples mainly contain

the δ form of mannitol. The fact that these samples have been lyophilized could explain this phase transition. Moreover, the δ polymorph of mannitol is one of the major phases in the optimized LNT sample. Additionally, the mannitol hemihydrate phase can also clearly be observed in this sample (and was also hinted in the blank sample) (Kulkarni, Suryanarayanan et al. 2018). Finally, the remaining reflections of the optimized LNT sample (indicated by asterisks in Figure 6) are most likely also originating from crystalline mannitol. Higuchi et al observed a similar phase when mannitol was mixed with large fractions of PVA (Higuchi, Tanaka et al. 2014). Possibly, also a combination of silymarin and PVA in the optimized LNT sample could trigger such a phase transformation of the mannitol.

3.2.5. Fourier transform infrared spectroscopy

FTIR spectra of pure drug, PVA, mannitol, physical mixture1 (mixing of pure SLM, mannitol and PVA), blank (lyophilized tablet without SLM), physical mixture2 (mixing of blank with pure SLM) and optimized LNT are shown in Figure 7. SLM spectrum illustrated the presence of a band of benzopyran ring vibrations at 1082 cm^{-1} with C—H at 823 cm^{-1} . Moreover, the reactive flavonolignan stretched ketone was at 1634.5 cm^{-1} accompanied with stretching vibrations of the aromatic ring was observed at 1510 cm^{-1} (Das, Roy et al. 2011). PVA spectrum showed the most characteristic band which is broad stretched band of O—H at 3295 cm^{-1} and vibrational band of C—H at 2908 cm^{-1} (Mansur, Sadahira et al. 2008). The spectrum of mannitol showed O-H and C-H stretching vibrations in the range between 3392 and 2902 cm^{-1} also another characteristic band for instance at $1418, 1301, 1209, 1078\text{ cm}^{-1}$ (Burger, Henck et al. 2000). While in the blank spectrum, δ -form of mannitol could be detected via its characteristic band for instance at $1452, 1377, 1333, 1249, 1084$ (Burger, Henck et al. 2000, Barreneche, Gil et al. 2013) that confirmed

the results of blank in DSC and PXRD. Moreover, the peak of PVA (3295 cm^{-1}) shifted towards lower wavenumbers (3196 cm^{-1}) due to intermolecular interaction between PVA and mannitol (Higuchi, Tanaka et al. 2014). On the other hand, the spectrum of the physical mixture² showed the distinctive peaks of SLM. While in the optimized LNT, the characteristic bands of the drug were observed and there was no significant difference between the physical mixture² and the optimized formula, which indicated absence of chemical interaction and thus the pharmacophore of the drug was not affected. On the other side, it may indicate physical interaction (intermolecular interaction) due to the formation of hydrogen bonds between the hydroxyl group of PVA and SLM molecule due to the characteristic band of the drug in the physical mixture² shift from 3253 cm^{-1} to 3197 cm^{-1} .

3.2.6. Stability Test

Results of the stability study are presented in Table 5. Stability studies showed that there is no significant difference in the mean particle size, zeta potential, friability, drug content and dissolution rate (T₉₀) before and after storage for 12 months ($p > 0.05$). The main particle size was slightly increased from 277.3 ± 10.3 to 295 ± 3.1 nm over 12 months as a result of steric stabilization based on nonionic polymer and, consequently, the dissolution rate was not affected during the storage period. The zeta potential was also unchanged, indicating no (chemical) alterations of the particle surfaces had taken place. Further, there was no significant difference in the disintegration time over 6 months ($p > 0.05$) while a difference of significance over a time period of 12 months ($p < 0.05$) was detected, but still within the limit (less than 30 seconds) according to FDA. Indeed, lyophilization generally play an important role in the physical and chemical stabilization of the drug (Abdelwahed, Degobert et al. 2006b). Furthermore, the highly

This is the accepted manuscript of [A.H. Ibrahim, E. Rosqvist, J.-H. Smått, H.M. Ibrahim, H.R. Ismael, M.I. Afouna, A.M. Samy, J.M. Rosenholm, Formulation and optimization of lyophilized nanosuspension tablets to improve the physicochemical properties and provide immediate release of silymarin. International Journal of Pharmaceutics 563 (2019) 217-227 <https://doi.org/10.1016/j.ijpharm.2019.03.064>] © 2019. This manuscript version is made available under the CC-BY-NC-ND 4.0 license <http://creativecommons.org/licenses/by-nc-nd/4.0/>”

porous structure of optimized LNT was maintained; which assured that the rapid disintegration and, consequently, high dissolution rate were also maintained during the storage period.

4. Conclusion

LNTs offer advantages of solving the problems encountered with the drug silymarin (SLM), associated with low water solubility, gastric degradation and consequently, low oral bioavailability. We demonstrated that incorporation and optimization of a nanosuspension technique tandem with lyophilized tablet in only one step is a promising formulation for achieving the optimum LNT. This was confirmed by studying the effect of the excipients PVA and mannitol on particle size, disintegration time, friability % and dissolution rate. The optimized LNTs are characterized by shorter disintegration time (less than 30 seconds) and lower friability (less than 1%) that fulfilled the pharmacopoeial requirements; i.e. particles in a stable nanosize range, faster dissolution rate, higher drug content and pronounced enhancement of saturation solubility. Therefore, these LNTs could be taken sublingually to bypass the gastric degradation and reach the systemic circulation directly and, consequently, the oral bioavailability would be significantly improved. Moreover, this formulation could be easily taken by geriatric patients or by anyone that may have difficulties in chewing or swallowing tablets or capsules.

Acknowledgements

This research was funded by Finnish National Agency for Education (Grant No. KM-18-10795) and partly by Academy of Finland (#309374).

This is the accepted manuscript of [A.H. Ibrahim, E. Rosqvist, J.-H. Smått, H.M. Ibrahim, H.R. Ismael, M.I. Afouna, A.M. Samy, J.M. Rosenholm, Formulation and optimization of lyophilized nanosuspension tablets to improve the physicochemical properties and provide immediate release of silymarin. International Journal of Pharmaceutics 563 (2019) 217-227 <https://doi.org/10.1016/j.ijpharm.2019.03.064>] © 2019. This manuscript version is made available under the CC-BY-NC-ND 4.0 license <http://creativecommons.org/licenses/by-nc-nd/4.0/>”

References

- Abdelwahed, W., et al. (2006a). "A pilot study of freeze drying of poly (epsilon-caprolactone) nanocapsules stabilized by poly (vinyl alcohol): formulation and process optimization." International journal of pharmaceutics **309**(1-2): 178-188.
- Abdelwahed, W., et al. (2006b). "Freeze-drying of nanoparticles: formulation, process and storage considerations." Advanced drug delivery reviews **58**(15): 1688-1713.
- Abrol, S., et al. (2004). "Formulation, characterization, and in vitro evaluation of silymarin-loaded lipid microspheres." Drug delivery **11**(3): 185-191.
- Ali, H. S., et al. (2011). "Hydrocortisone nanosuspensions for ophthalmic delivery: a comparative study between microfluidic nanoprecipitation and wet milling." Journal of Controlled Release **149**(2): 175-181.
- Balata, G. and H. Shamrool (2014). "Spherical agglomeration versus solid dispersion as different trials to optimize dissolution and bioactivity of silymarin." Journal of Drug Delivery Science and Technology **24**(5): 478-485.
- Barreneche, C., et al. (2013). "Effect of d-mannitol polymorphism in its thermal energy storage capacity when it is used as PCM." Solar Energy **94**: 344-351.
- Bhattacharjee, S. (2016). "DLS and zeta potential—What they are and what they are not?" Journal of Controlled Release **235**: 337-351.
- Brough, C. and R. Williams Iii (2013). "Amorphous solid dispersions and nano-crystal technologies for poorly water-soluble drug delivery." International Journal of Pharmaceutics **453**(1): 157-166.
- Burger, A., et al. (2000). "Energy/temperature diagram and compression behavior of the polymorphs of D-mannitol." Journal of pharmaceutical sciences **89**(4): 457-468.
- Cao, X., et al. (2012). "Oral bioavailability of silymarin formulated as a novel 3-day delivery system based on porous silica nanoparticles." Acta biomaterialia **8**(6): 2104-2112.

This is the accepted manuscript of [A.H. Ibrahim, E. Rosqvist, J.-H. Smått, H.M. Ibrahim, H.R. Ismael, M.I. Afouna, A.M. Samy, J.M. Rosenholm, Formulation and optimization of lyophilized nanosuspension tablets to improve the physicochemical properties and provide immediate release of silymarin. International Journal of Pharmaceutics 563 (2019) 217-227 <https://doi.org/10.1016/j.ijpharm.2019.03.064>] © 2019. This manuscript version is made available under the CC-BY-NC-ND 4.0 license <http://creativecommons.org/licenses/by-nc-nd/4.0/>”

Cengiz, M., et al. (2015). "A comparative study on the therapeutic effects of silymarin and silymarin-loaded solid lipid nanoparticles on d-GalN/TNF- α -induced liver damage in balb/c mice." Food and Chemical Toxicology **77**: 93-100.

Chu, C., et al. (2011). "Proliposomes for oral delivery of dehydrosilymarin: preparation and evaluation in vitro and in vivo." Acta pharmacologica sinica **32**(7): 973.

Corveleyn, S. and J. P. Remon (1997). "Formulation and production of rapidly disintegrating tablets by lyophilisation using hydrochlorothiazide as a model drug." International Journal of Pharmaceutics **152**(2): 215-225.

Ćurić, A., et al. (2015). "Development and lyophilization of itraconazole loaded poly (butyl cyanoacrylate) nanospheres as a drug delivery system." European Journal of Pharmaceutical Sciences **78**: 121-131.

Das, S., et al. (2011). "Silymarin nanoparticle prevents paracetamol-induced hepatotoxicity." International journal of nanomedicine **6**: 1291.

De Waard, H., et al. (2008). "A novel bottom-up process to produce drug nanocrystals: controlled crystallization during freeze-drying." Journal of Controlled Release **128**(2): 179-183.

Dening, T. J., et al. (2016). "Oral nanomedicine approaches for the treatment of psychiatric illnesses." Journal of Controlled Release **223**: 137-156.

Du, J., et al. (2015). "Nanosuspensions of poorly water-soluble drugs prepared by bottom-up technologies." International Journal of Pharmaceutics **495**(2): 738-749.

El-Samaligy, M., et al. (2006). "Increasing bioavailability of silymarin using a buccal liposomal delivery system: preparation and experimental design investigation." International journal of pharmaceutics **308**(1-2): 140-148.

Elmowafy, M., et al. (2013). "Silymarin loaded liposomes for hepatic targeting: in vitro evaluation and HepG2 drug uptake." European Journal of Pharmaceutical Sciences **50**(2): 161-171.

FDA (2003). "Guidance for Industry: Q1A(R2) Stability Testing of New Drug Substances and Products, U.S. Department of Health and Human Services, Food and Drug Administration." 1-22.

This is the accepted manuscript of [A.H. Ibrahim, E. Rosqvist, J.-H. Smått, H.M. Ibrahim, H.R. Ismael, M.I. Afouna, A.M. Samy, J.M. Rosenholm, Formulation and optimization of lyophilized nanosuspension tablets to improve the physicochemical properties and provide immediate release of silymarin. International Journal of Pharmaceutics 563 (2019) 217-227 <https://doi.org/10.1016/j.ijpharm.2019.03.064>] © 2019. This manuscript version is made available under the CC-BY-NC-ND 4.0 license <http://creativecommons.org/licenses/by-nc-nd/4.0/>”

Flora, K., et al. (1998). "Milk thistle (*Silybum marianum*) for the therapy of liver disease." The American journal of gastroenterology **93**(2): 139.

Fonte, P., et al. (2016). "Facts and evidences on the lyophilization of polymeric nanoparticles for drug delivery." Journal of Controlled Release **225**: 75-86.

Ghosh, A., et al. (2011). "Preparation and evaluation of silymarin β -cyclodextrin molecular inclusion complexes." Journal of young pharmacists: JYP **3**(3): 205.

Gil, A., et al. (2013). "Thermal behaviour of d-mannitol when used as PCM: Comparison of results obtained by DSC and in a thermal energy storage unit at pilot plant scale." Applied energy **111**: 1107-1113.

Gittings, S., et al. (2014). "Dissolution methodology for taste masked oral dosage forms." Journal of Controlled Release **173**: 32-42.

Higuchi, M., et al. (2014). "Hygroscopicity of a sugarless coating layer formed by the interaction between mannitol and poly (vinyl alcohol)(PVA)." Colloids and Surfaces B: Biointerfaces **123**: 557-565.

Ibrahim, A. H., et al. (2018). "Optimization and evaluation of lyophilized fenofibrate nanoparticles with enhanced oral bioavailability and efficacy." Pharmaceutical development and technology **23**(4): 358-369.

Ige, P. P., et al. (2013). "Fabrication of fenofibrate nanocrystals by probe sonication method for enhancement of dissolution rate and oral bioavailability." Colloids and Surfaces B: Biointerfaces **108**: 366-373.

Kayaert, P. and G. Van den Mooter (2012). "Is the amorphous fraction of a dried nanosuspension caused by milling or by drying? A case study with Naproxen and Cinnarizine." European Journal of Pharmaceutics and Biopharmaceutics **81**(3): 650-656.

Kulkarni, S. S., et al. (2018). "Mechanisms by which crystalline mannitol improves the reconstitution time of high concentration lyophilized protein formulations." European Journal of Pharmaceutics and Biopharmaceutics **131**: 70-81.

Kvasnička, F., et al. (2003). "Analysis of the active components of silymarin." Journal of Chromatography A **990**(1-2): 239-245.

This is the accepted manuscript of [A.H. Ibrahim, E. Rosqvist, J.-H. Smått, H.M. Ibrahim, H.R. Ismael, M.I. Afouna, A.M. Samy, J.M. Rosenholm, Formulation and optimization of lyophilized nanosuspension tablets to improve the physicochemical properties and provide immediate release of silymarin. International Journal of Pharmaceutics 563 (2019) 217-227 <https://doi.org/10.1016/j.ijpharm.2019.03.064>] © 2019. This manuscript version is made available under the CC-BY-NC-ND 4.0 license <http://creativecommons.org/licenses/by-nc-nd/4.0/>”

Li, X., et al. (2010). "Development of silymarin self-microemulsifying drug delivery system with enhanced oral bioavailability." Aaps Pharmscitech **11**(2): 672-678.

Lian, R., et al. (2011). "Silymarin glyceryl monooleate/poloxamer 407 liquid crystalline matrices: physical characterization and enhanced oral bioavailability." Aaps Pharmscitech **12**(4): 1234-1240.

Lu, C., et al. (2007). "Synchronized and sustained release of multiple components in silymarin from erodible glyceryl monostearate matrix system." European journal of pharmaceutics and biopharmaceutics **66**(2): 210-219.

Mahesh, K. V., et al. (2014). "A comparative study of top-down and bottom-up approaches for the preparation of nanosuspensions of glipizide." Powder Technology **256**: 436-449.

Malamatari, M., et al. (2016). "Solidification of nanosuspensions for the production of solid oral dosage forms and inhalable dry powders." Expert opinion on drug delivery **13**(3): 435-450.

Mansur, H. S., et al. (2008). "FTIR spectroscopy characterization of poly (vinyl alcohol) hydrogel with different hydrolysis degree and chemically crosslinked with glutaraldehyde." Materials Science and Engineering: C **28**(4): 539-548.

McLaughlin, R., et al. (2009). "Orally disintegrating tablets: the effect of recent FDA guidance on ODT technologies and applications."

Mehta, M., et al. (2013). "Controlling the physical form of mannitol in freeze-dried systems." European Journal of Pharmaceutics and Biopharmaceutics **85**(2): 207-213.

Merisko-Liversidge, E. and G. G. Liversidge (2011). "Nanosizing for oral and parenteral drug delivery: a perspective on formulating poorly-water soluble compounds using wet media milling technology." Advanced drug delivery reviews **63**(6): 427-440.

Morakul, B., et al. (2013). "Precipitation-lyophilization-homogenization (PLH) for preparation of clarithromycin nanocrystals: Influencing factors on physicochemical properties and stability." International Journal of Pharmaceutics **457**(1): 187-196.

This is the accepted manuscript of [A.H. Ibrahim, E. Rosqvist, J.-H. Smått, H.M. Ibrahim, H.R. Ismael, M.I. Afouna, A.M. Samy, J.M. Rosenholm, Formulation and optimization of lyophilized nanosuspension tablets to improve the physicochemical properties and provide immediate release of silymarin. International Journal of Pharmaceutics 563 (2019) 217-227 <https://doi.org/10.1016/j.ijpharm.2019.03.064>] © 2019. This manuscript version is made available under the CC-BY-NC-ND 4.0 license <http://creativecommons.org/licenses/by-nc-nd/4.0/>”

Möschwitzer, J. P. (2013). "Drug nanocrystals in the commercial pharmaceutical development process." International Journal of Pharmaceutics **453**(1): 142-156.

Mou, D., et al. (2011). "Potent dried drug nanosuspensions for oral bioavailability enhancement of poorly soluble drugs with pH-dependent solubility." International Journal of Pharmaceutics **413**(1-2): 237-244.

Parveen, R., et al. (2011). "Oil based nanocarrier for improved oral delivery of silymarin: in vitro and in vivo studies." International Journal of Pharmaceutics **413**(1-2): 245-253.

Rabinow, B. E. (2004). "Nanosuspensions in drug delivery." Nature reviews Drug discovery **3**(9): 785.

Rana, P. and R. Murthy (2013). "Formulation and evaluation of mucoadhesive buccal films impregnated with carvedilol nanosuspension: a potential approach for delivery of drugs having high first-pass metabolism." Drug delivery **20**(5): 224-235.

Sinha, B., et al. (2013). "Bottom-up approaches for preparing drug nanocrystals: formulations and factors affecting particle size." International Journal of Pharmaceutics **453**(1): 126-141.

Solé, A., et al. (2014). "Thermal stability test of sugar alcohols as phase change materials for medium temperature energy storage application." Energy Procedia **48**: 436-439.

Sun, N., et al. (2008). "Enhanced dissolution of silymarin/polyvinylpyrrolidone solid dispersion pellets prepared by a one-step fluid-bed coating technique." Powder Technology **182**(1): 72-80.

Tran, T. T.-D., et al. (2014). "Amorphous isradipine nanosuspension by the sonoprecipitation method." International Journal of Pharmaceutics **474**(1-2): 146-150.

Van Eerdenbrugh, B., et al. (2008). "Drying of crystalline drug nanosuspensions—the importance of surface hydrophobicity on dissolution behavior upon redispersion." European Journal of Pharmaceutical Sciences **35**(1-2): 127-135.

Verma, S., et al. (2009). "Quality by design approach to understand the process of nanosuspension preparation." International Journal of Pharmaceutics **377**(1-2): 185-198.

This is the accepted manuscript of [A.H. Ibrahim, E. Rosqvist, J.-H. Smått, H.M. Ibrahim, H.R. Ismael, M.I. Afouna, A.M. Samy, J.M. Rosenholm, Formulation and optimization of lyophilized nanosuspension tablets to improve the physicochemical properties and provide immediate release of silymarin. International Journal of Pharmaceutics 563 (2019) 217-227 <https://doi.org/10.1016/j.ijpharm.2019.03.064>] © 2019. This manuscript version is made available under the CC-BY-NC-ND 4.0 license <http://creativecommons.org/licenses/by-nc-nd/4.0/>”

Wang, Y., et al. (2011). "Development and in vitro evaluation of deacety mycoepoxydiene nanosuspension." Colloids and Surfaces B: Biointerfaces **83**(2): 189-197.

Wilkhu, J. S., et al. (2017). "Development of a solid dosage platform for the oral delivery of bilayer vesicles." European Journal of Pharmaceutical Sciences **108**: 71-77.

Wu, W., et al. (2006). "Enhanced bioavailability of silymarin by self-microemulsifying drug delivery system." European Journal of Pharmaceutics and Biopharmaceutics **63**(3): 288-294.

Yanyu, X., et al. (2006). "The preparation of silybin–phospholipid complex and the study on its pharmacokinetics in rats." International Journal of Pharmaceutics **307**(1): 77-82.

Zhang, J., et al. (2007). "Preparation and characterization of solid lipid nanoparticles containing silibinin." Drug delivery **14**(6): 381-387.

This is the accepted manuscript of [A.H. Ibrahim, E. Rosqvist, J.-H. Smått, H.M. Ibrahim, H.R. Ismael, M.I. Afouna, A.M. Samy, J.M. Rosenholm, Formulation and optimization of lyophilized nanosuspension tablets to improve the physicochemical properties and provide immediate release of silymarin. International Journal of Pharmaceutics 563 (2019) 217-227 <https://doi.org/10.1016/j.ijpharm.2019.03.064>] © 2019. This manuscript version is made available under the CC-BY-NC-ND 4.0 license <http://creativecommons.org/licenses/by-nc-nd/4.0/>”

Table 1. 3² full factorial design with observed response values of lyophilized nanosuspension tablet.

Batch Code	Independent variables				Dependent variables				Goal
	PVA concentration (X1)		Mannitol concentration (X2)		Particles size (After lyophilization) (Y1)	Disintegration time (Y2)	Friability (Y3)	T90 (Y4)	Minimize
	%w/v	level	%w/v	Level	nm	second	%	minute	
N1	1	—1	1	—1	546.5± 68.4	7.3± 2.4	2.5	29.6±6.5	
N2	2	0	1	—1	421.2±8.1	65.0 ± 3.0	0.4	25.6±2.5	
N3	3	1	1	—1	427.8±14.45	125.0 ± 4.1	0.08	44.2±3.8	
N4	1	—1	5	0	405.8±17.5	2.3± 0.7	4.9	20.8±0.8	
N5	2	0	5	0	277.6± 6.1	22.3± 3.0	0.8	11.1±0.5	
N6	3	1	5	0	299.4±8.3	45± 2.4	0.14	30.4±0.9	
N7	1	—1	9	1	339.6±4.8	1.6± 0.4	6.3	15.5 ±1.0	
N8	2	0	9	1	269.7±1.8	12± 1.6	1.1	7.1 ±0.2	
N9	3	1	9	1	316.7±5.7	22.6± 2.0	0.13	20.8 ±2.0	

This is the accepted manuscript of [A.H. Ibrahim, E. Rosqvist, J.-H. Smått, H.M. Ibrahim, H.R. Ismael, M.I. Afouna, A.M. Samy, J.M. Rosenholm, Formulation and optimization of lyophilized nanosuspension tablets to improve the physicochemical properties and provide immediate release of silymarin. International Journal of Pharmaceutics 563 (2019) 217-227 <https://doi.org/10.1016/j.ijpharm.2019.03.064>] © 2019. This manuscript version is made available under the CC-BY-NC-ND 4.0 license <http://creativecommons.org/licenses/by-nc-nd/4.0/>”

Table 2. Analysis of variance for dependent variables of 3² FFD

Source	Sum of Squares	Df	Mean Square	F-Ratio	P-Value	R ² value
<i>Mean Particle Size (Y1)</i>						99.3%
Model	65117.99	5	13023.60	79.61	0.0022	
X ₁	10184.6	1	10184.6	62.26	0.0042	
X ₂	36738.4	1	36738.4	224.58	0.0006	
X ₁ ²	8800.22	1	8800.22	53.79	0.0052	
X ₁ X ₂	2294.41	1	2294.41	14.03	0.0332	
X ₂ ²	7100.35	1	7100.35	43.4	0.0071	
<i>Disintegration time (Y2)</i>						98.2 %
Model	12643.11	5	2528.62	31.96	0.0084	
X ₁	5484.33	1	5484.33	69.32	0.0036	
X ₂	4325.54	1	4325.54	54.67	0.0051	
X ₁ ²	1.502	1	1.50	0.02	0.8991	
X ₁ X ₂	2337.72	1	2337.72	29.55	0.0122	
X ₂ ²	494.03	1	494.03	6.24	0.0878	
<i>Friability (Y3)</i>						98.6%
Model	41.71	5	8.34	42.18	0.0056	
X ₁	29.70	1	29.70	150.19	0.0012	
X ₂	3.45	1	3.45	17.45	0.025	
X ₁ ²	4.96	1	4.96	25.09	0.0153	
X ₁ X ₂	3.52	1	3.52	17.78	0.0244	
X ₂ ²	0.076	1	0.076	0.38	0.5791	
<i>time to 90% drug release (Y4)</i>						99.5%
Model	1009.49	5	201.90	121.74	0.0012	
X ₁	145.04	1	145.04	87.46	0.0026	
X ₂	522.67	1	522.67	315.16	0.0004	
X ₁ ²	301.76	1	301.76	181.96	0.0009	
X ₁ X ₂	21.62	1	21.62	13.04	0.0365	
X ₂ ²	18.40	1	18.40	11.1	0.0447	

This is the accepted manuscript of [A.H. Ibrahim, E. Rosqvist, J.-H. Smått, H.M. Ibrahim, H.R. Ismael, M.I. Afouna, A.M. Samy, J.M. Rosenholm, Formulation and optimization of lyophilized nanosuspension tablets to improve the physicochemical properties and provide immediate release of silymarin. International Journal of Pharmaceutics 563 (2019) 217-227 <https://doi.org/10.1016/j.ijpharm.2019.03.064>] © 2019. This manuscript version is made available under the CC-BY-NC-ND 4.0 license <http://creativecommons.org/licenses/by-nc-nd/4.0/>”

Table 3. Results of mean particle size after and before lyophilization and the mechanical strength for the nine batches

Formula	N1	N2	N3	N4	N5	N6	N7	N8	N9
Particle size before lyophilization (nm)	236 ± 3.1	247.8 ± 4.3	297.3 ± 3.17	230.4 ± 0.9	255.2 ± 3.8	289.9 ± 5.9	239.9 ± 0.8	248.0 ± 5.3	298.1 ± 6.6
Particle size after lyophilization (nm)	546.5 ± 68.4	421.2 ± 8.1	427.8 ± 14.45	405.8 ± 17.5	277.6 ± 6.1	299.4 ± 8.3	339.6 ± 4.8	269.7 ± 1.8	316.7 ± 5.7
Tablet strength (g)	76.6 ± 9.8	171.4 ± 15.3	362.4 ± 23.9	113.1 ± 13.4	281.7 ± 31.5	498.7 ± 44.7	101.7 ± 7.7	402.3 ± 18.0	654.5 ± 47.2

This is the accepted manuscript of [A.H. Ibrahim, E. Rosqvist, J.-H. Smått, H.M. Ibrahim, H.R. Ismael, M.I. Afouna, A.M. Samy, J.M. Rosenholm, Formulation and optimization of lyophilized nanosuspension tablets to improve the physicochemical properties and provide immediate release of silymarin. International Journal of Pharmaceutics 563 (2019) 217-227 <https://doi.org/10.1016/j.ijpharm.2019.03.064>] © 2019. This manuscript version is made available under the CC-BY-NC-ND 4.0 license <http://creativecommons.org/licenses/by-nc-nd/4.0/>”

Table 4. Illustration of predicted and observed values for all responses with their relative errors.

Responses	predicted values	observed values	Relative error (%)
mean particle size (Y1) nm	266	277.3± 10.4	4.2
Disintegration time (Y2) second	13.6	14.0 ± 2.2	3.7
Friability (Y3) %	0.57	0.59± 0.07	3.5
T90 (Y4) minute	8.6	8.9± 0.6	3.4

Table 5. Results of stability study

Characterization	Initial	1 month	2 month	3 month	6 months	12 months
Mean particle size(nm) ± SD	277.3 ±10.3	279.3 ±8.5	286.9± 4.1	290.5 ± 13.1	292.3 ± 5.6	295 ± 3.1
Zeta potential (mV) ±SD	−22.8 ± 2.8	−22.2 ± 0.8	−21.0 ± 0.5	−21.3 ± 0.4	−21.6 ± 0.1	−21.2±0.5
T ₉₀ (min.)	8.9± 0.6	10.4 ± 0.8	11 ± 1.1	11.5 ± 1.5	13.7 ± 2.9	15.7 ± 3.4
Drug content(%)± SD	96.8 ±1.85	96.5 ± 1.5	96.0 ± 2.4	96.2 ± 1.4	96.1 ± 2.7	95.8 ± 2.8
Disintegration time (sec.) ±SD	14.0± 2.2	15.3 ±1.8	16.2± 2.1	17.2 ± 2.5	19.3 ± 2.9	22.0 ± 3.8
Friability (%)	0.61± 0.09	0.58 ± 0.05	0.57± 0.05	0.53± 0.1	0.5 ± 0.06	0.46 ± 0.02

This is the accepted manuscript of [A.H. Ibrahim, E. Rosqvist, J.-H. Smått, H.M. Ibrahim, H.R. Ismael, M.I. Afouna, A.M. Samy, J.M. Rosenholm, Formulation and optimization of lyophilized nanosuspension tablets to improve the physicochemical properties and provide immediate release of silymarin. International Journal of Pharmaceutics 563 (2019) 217-227 <https://doi.org/10.1016/j.ijpharm.2019.03.064>] © 2019. This manuscript version is made available under the CC-BY-NC-ND 4.0 license <http://creativecommons.org/licenses/by-nc-nd/4.0/>”

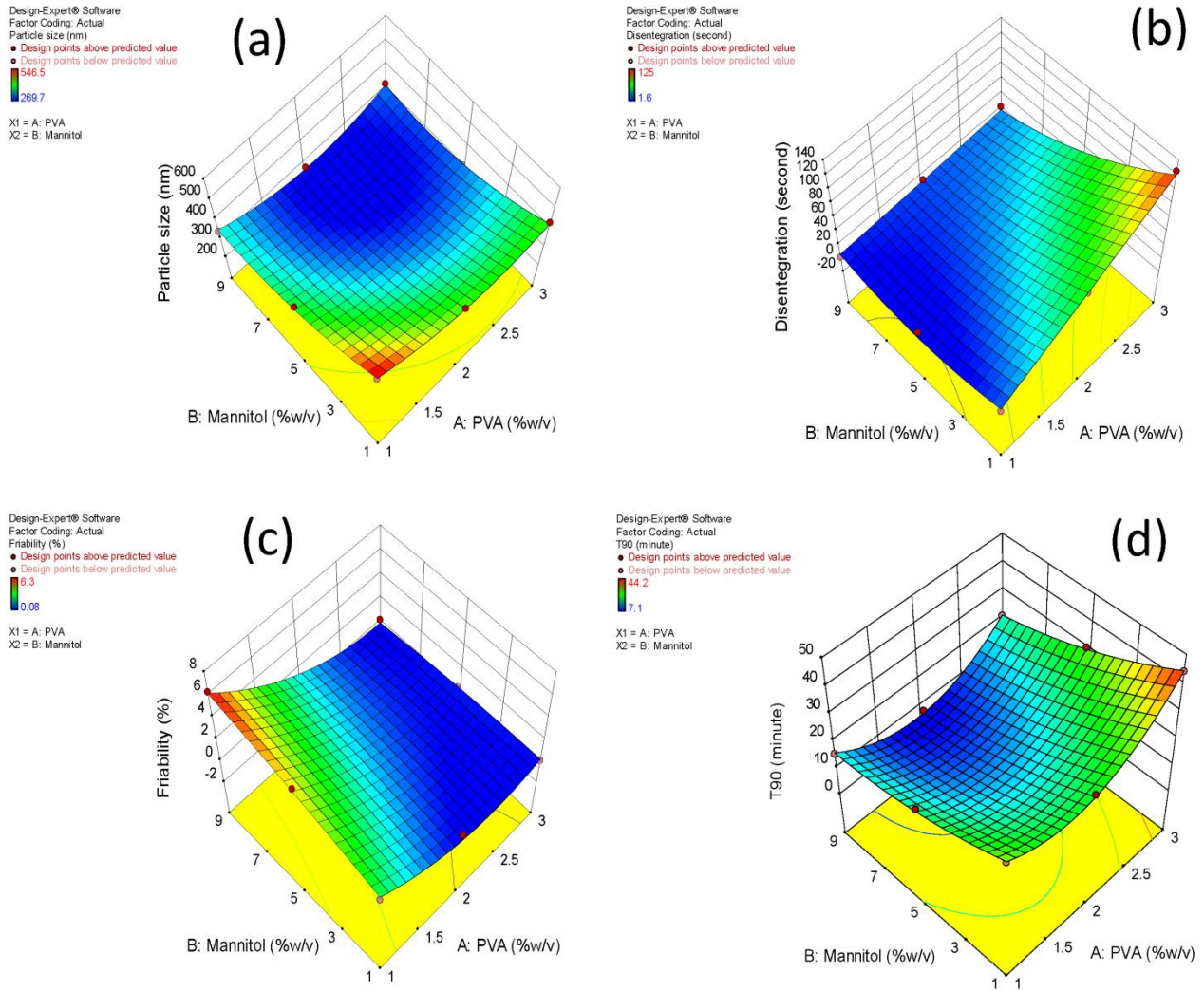


Figure 1.

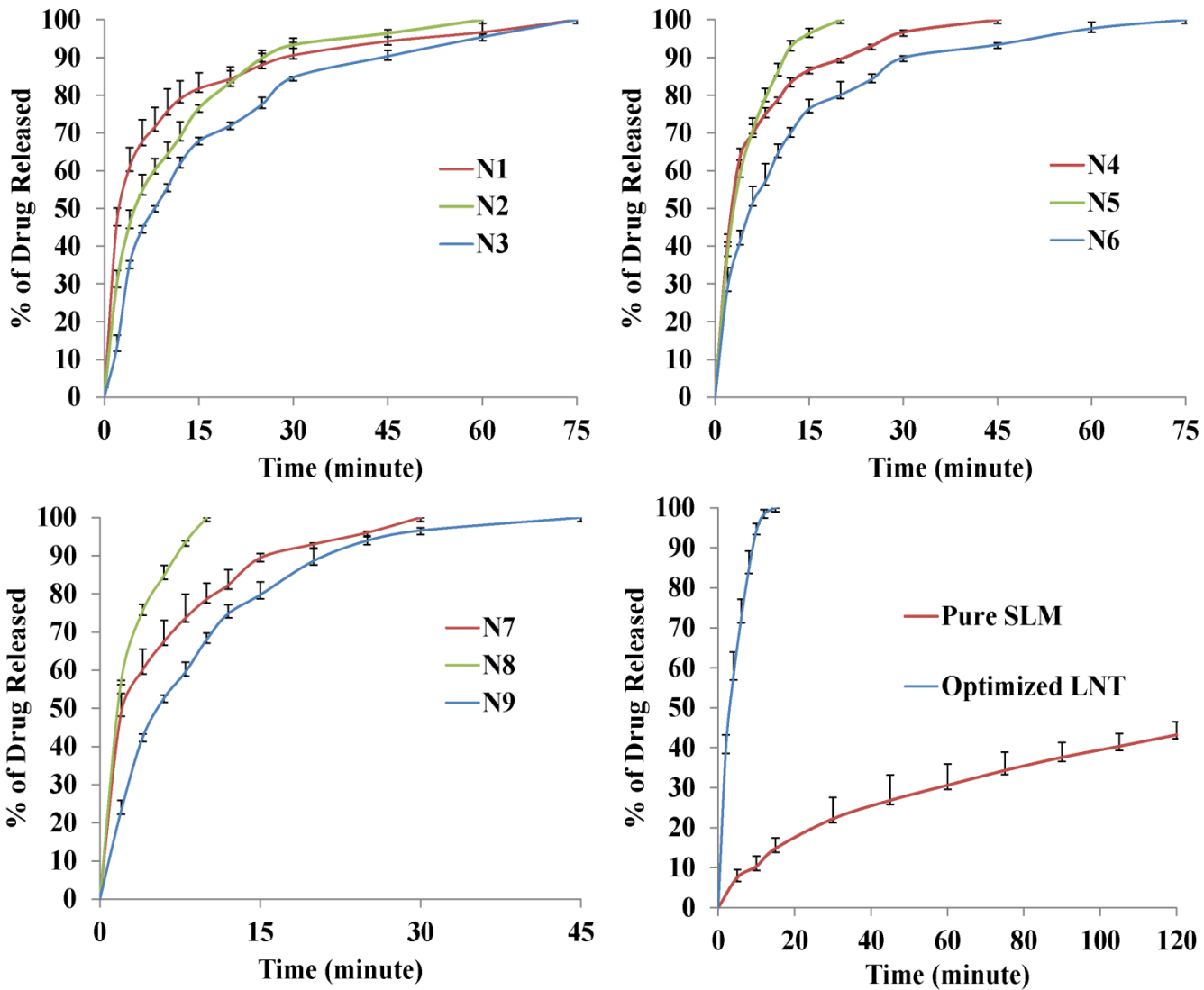


Figure 2.

Design-Expert® Software
Factor Coding: Actual
Desirability
1.000
0.000
X1 = A: PVA
X2 = B: Mannitol

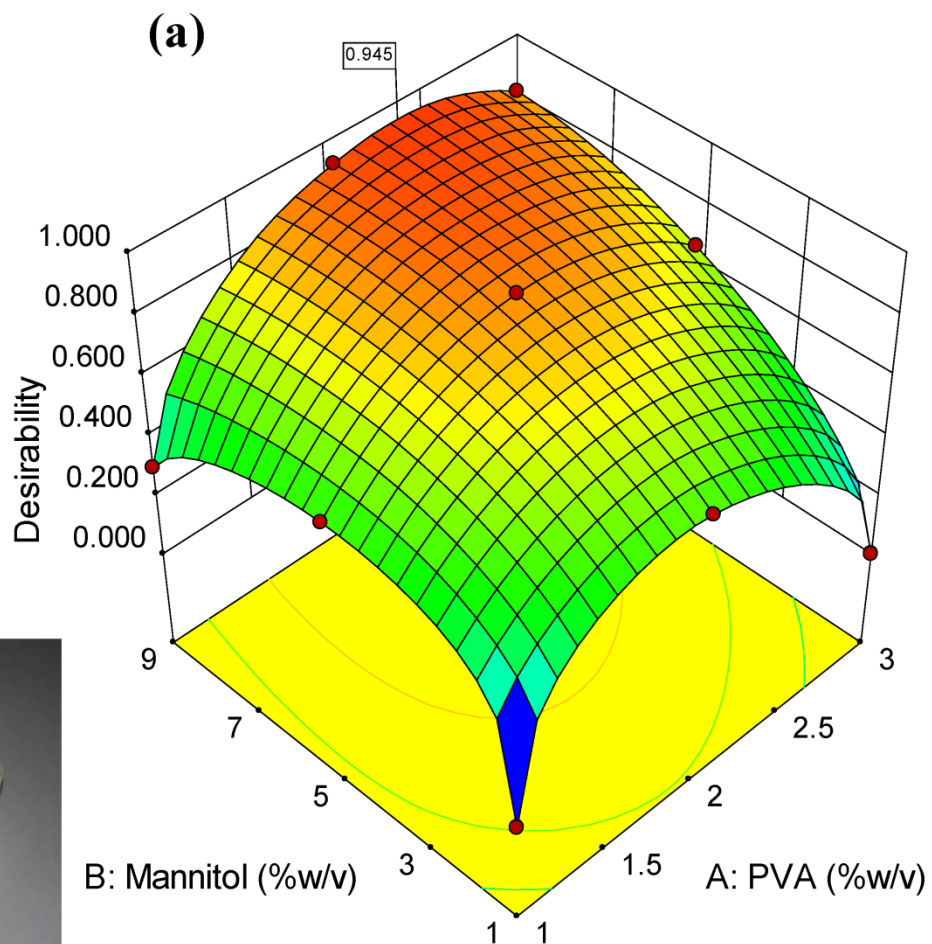
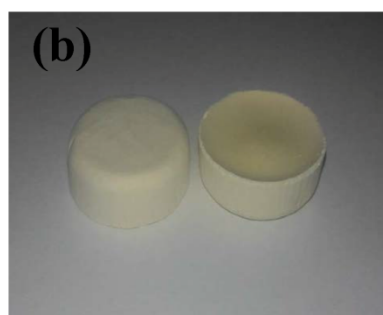


Figure 3.

This is the accepted manuscript of [A.H. Ibrahim, E. Rosqvist, J.-H. Smått, H.M. Ibrahim, H.R. Ismael, M.I. Afouna, A.M. Samy, J.M. Rosenholm, Formulation and optimization of lyophilized nanosuspension tablets to improve the physicochemical properties and provide immediate release of silymarin. International Journal of Pharmaceutics 563 (2019) 217-227 <https://doi.org/10.1016/j.ijpharm.2019.03.064>] © 2019. This manuscript version is made available under the CC-BY-NC-ND 4.0 license <http://creativecommons.org/licenses/by-nc-nd/4.0/>”

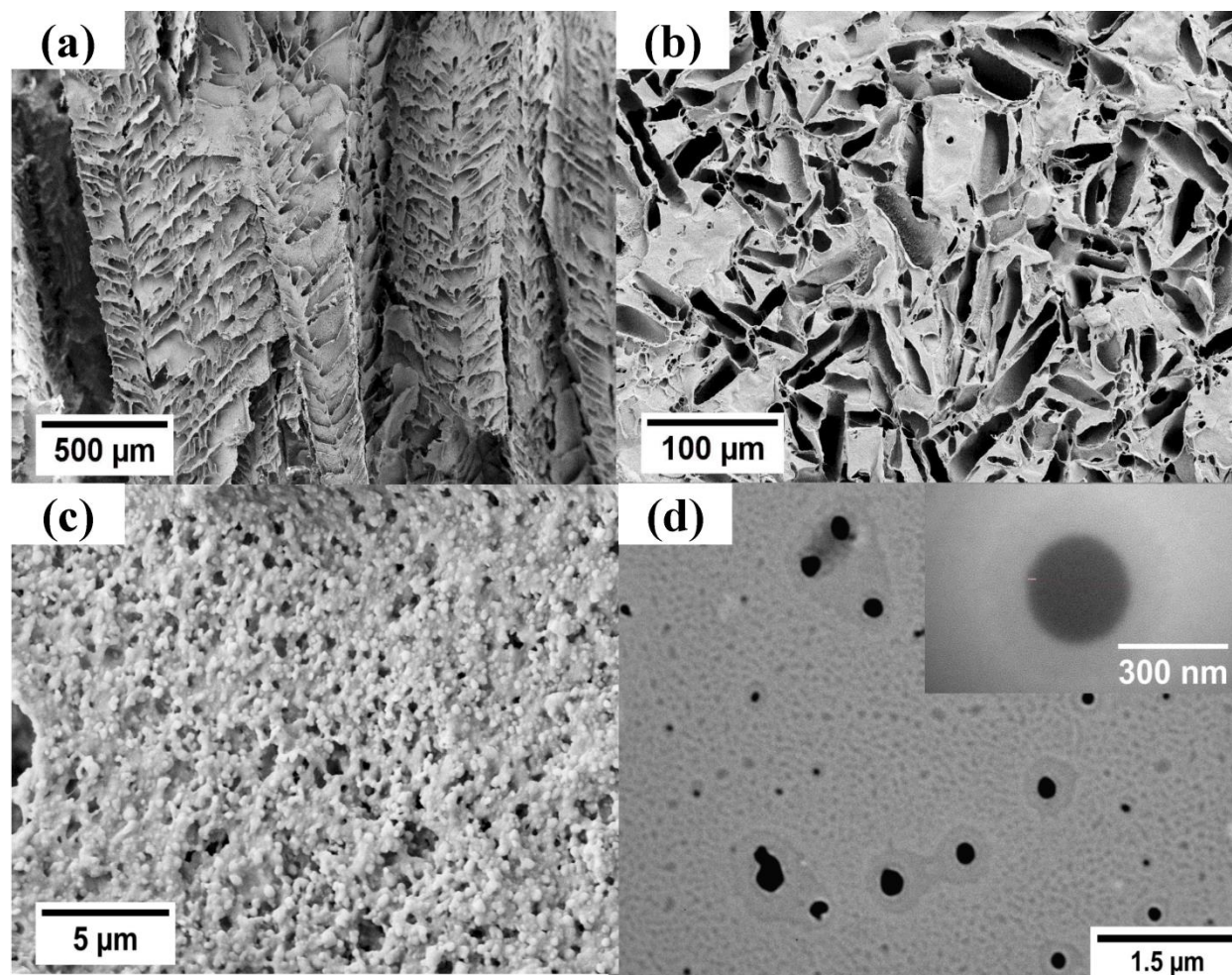


Figure 4.

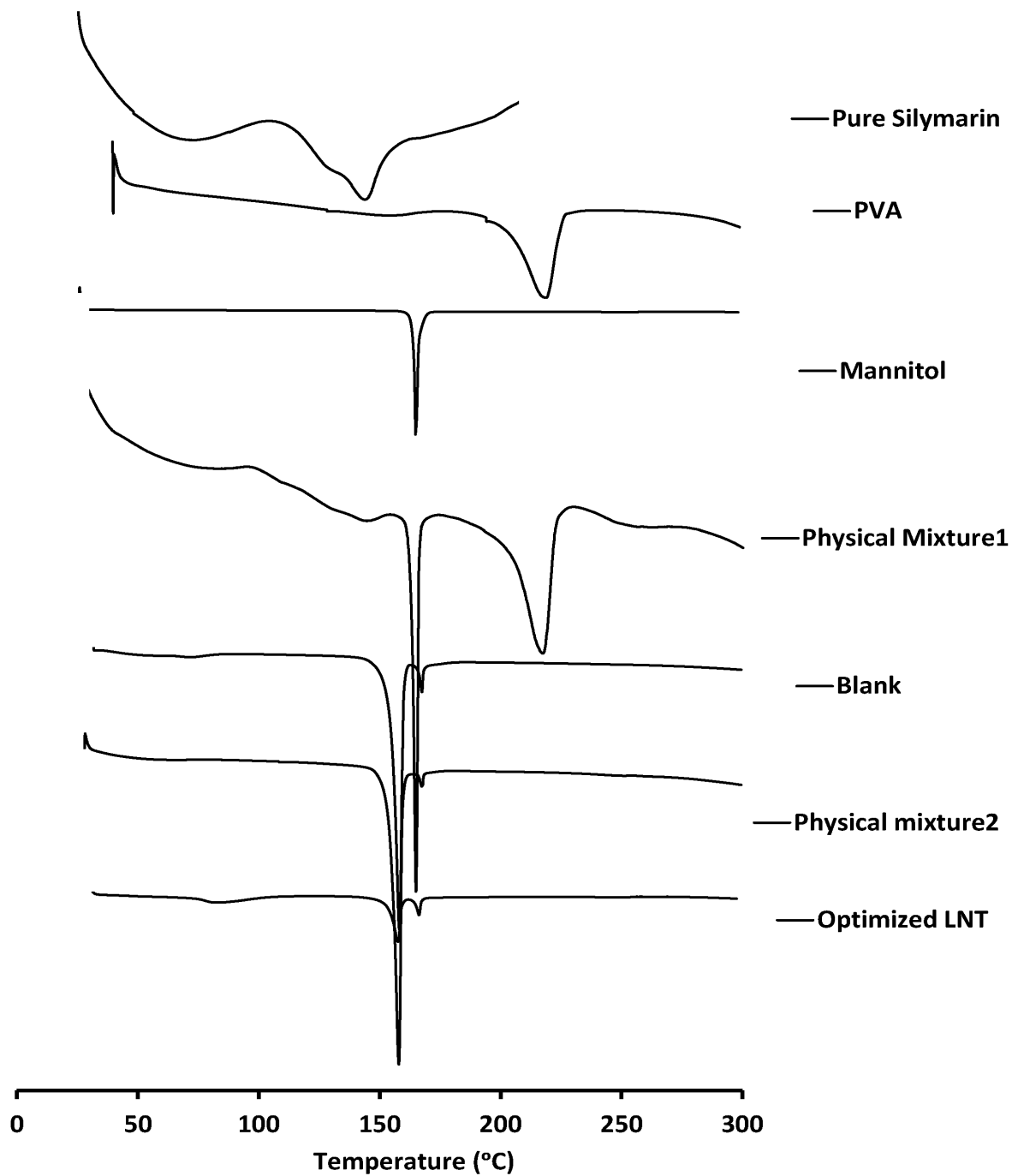


Figure 5.

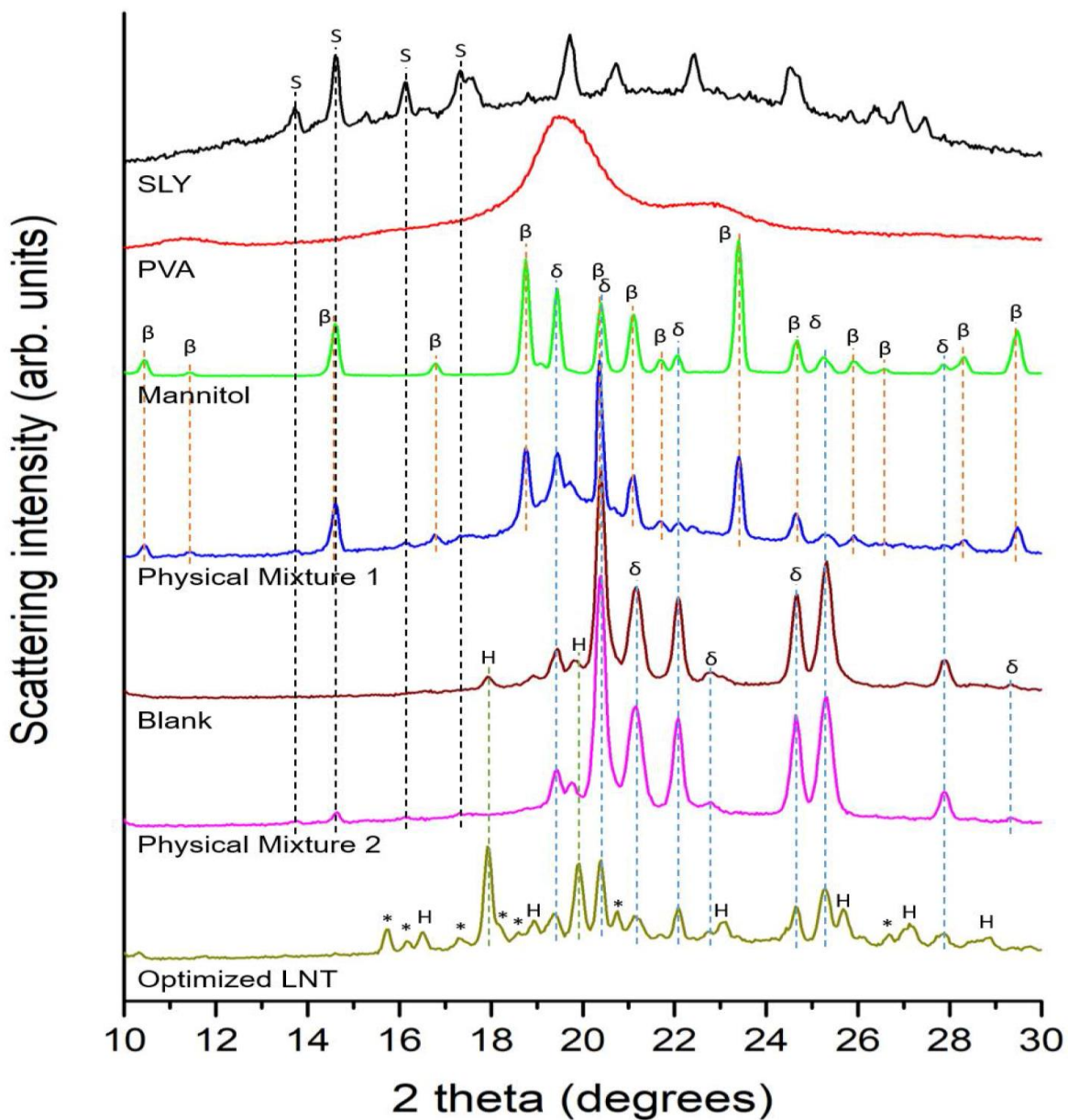


Figure 6.

This is the accepted manuscript of [A.H. Ibrahim, E. Rosqvist, J.-H. Smått, H.M. Ibrahim, H.R. Ismael, M.I. Afouna, A.M. Samy, J.M. Rosenholm, Formulation and optimization of lyophilized nanosuspension tablets to improve the physicochemical properties and provide immediate release of silymarin. International Journal of Pharmaceutics 563 (2019) 217-227 <https://doi.org/10.1016/j.ijpharm.2019.03.064>] © 2019. This manuscript version is made available under the CC-BY-NC-ND 4.0 license <http://creativecommons.org/licenses/by-nc-nd/4.0/>”

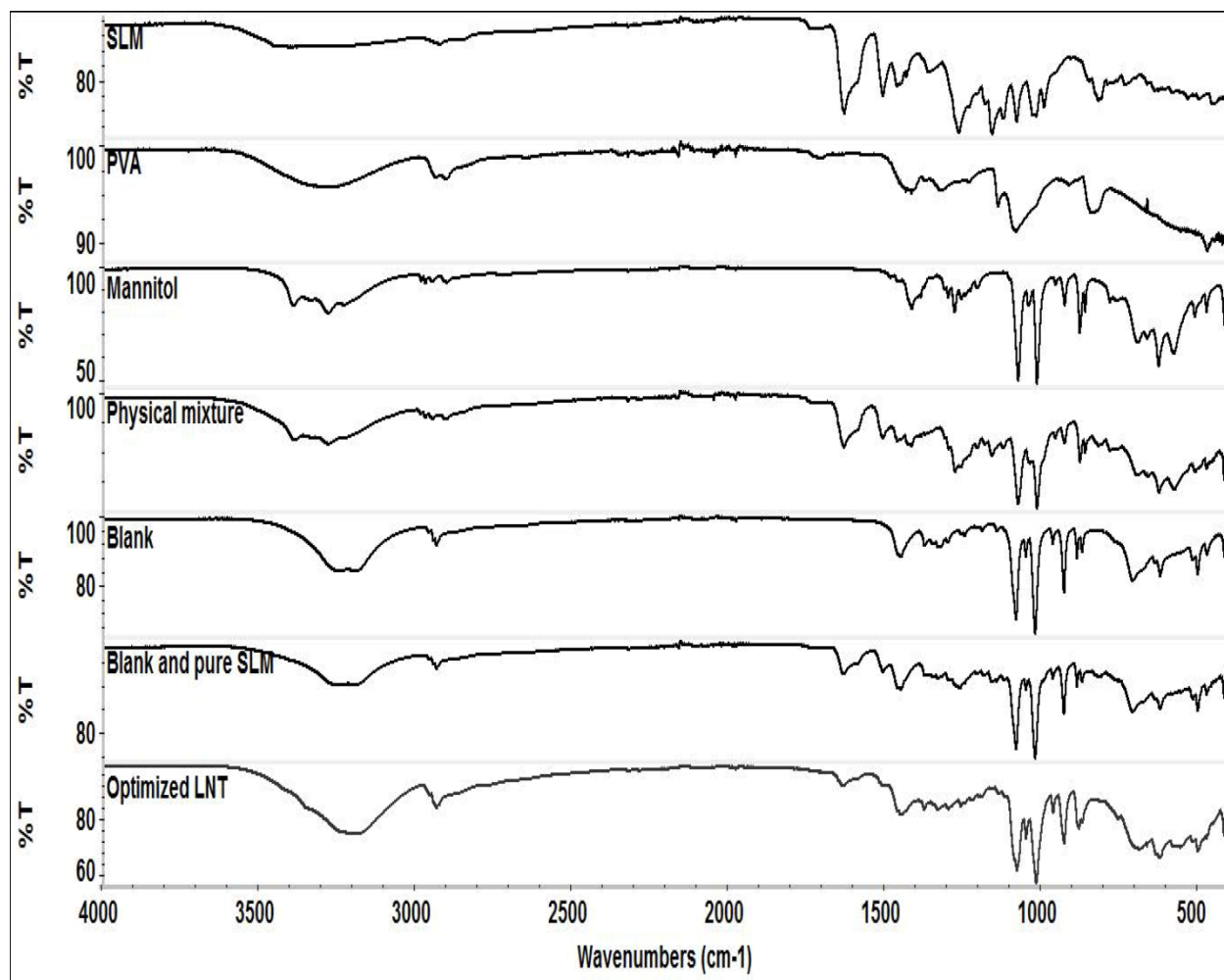


Figure 7.

Figure Legends

Figure 1. 3D graphs of response surface showing the effect of both independent variables (PVA and mannitol) on (a) mean particle size, (b) In vitro disintegration time, (c) Friability % and (d) T90.

Figure 2. Dissolution profiles pure SLM, nine batches, and optimized LNT.

Figure 3. (a) Optimization of LNT through desirability plot and (b) image of optimized LNT.

Figure 4. Different view of SEM micrograph for optimized LNT (a) cross-sectional view, (b) surface view and (c) higher magnification of SEM micrograph. (d) TEM image for optimized LNT.

Figure 5. DSC thermograms for pure SLM, PVA, Mannitol, physical mixture1, blank, physical mixture2 and optimized LNT.

Figure 6. PXRD patterns for pure SLM, PVA, Mannitol, physical mixture1, blank, physical mixture2 and optimized LNT.

Figure 7. FTIR spectra pure SLM, PVA, Mannitol, physical mixture1, blank, physical mixture2 and optimized LNT.